



The new buckling curves for cold-formed stainless steel equal-leg angle columns*

Jelena Dobrić¹⁾, Aljoša Filipović¹⁾, Nancy Baddoo²⁾, Zlatko Marković¹⁾, Dragan Buđevac¹⁾

¹⁾ University of Belgrade Faculty of Civil Engineering, Bulevar kralja Aleksandra 73, 11000 Belgrade, Serbia

²⁾ Steel Construction Institute United Kingdom

Article history

Received: 27 July 2021

Received in revised form: /

Accepted: 30 August 2021

Available online: 30 September 2021

Keywords

stainless steel,
cold-formed angle section,
flexural buckling,
flexural-torsional buckling,
buckling curves,
design

ABSTRACT

The design rules for centrally compressed stainless steel equal-leg angle members are not explicitly stated in the current European standard SRPS EN 1993-1-4. This paper summarizes the results of extensive research conducted on this type of structural elements aiming to define recommendations for their design. Based on a systematic experimental investigation, a detailed numerical analysis was performed, and a database of columns' resistances were defined. Material and geometric nonlinear analysis included three key stainless steel alloys, austenitic, ferritic and duplex. The design curves for flexural and flexural-torsional buckling check have been proposed in accordance with European codified procedures.

1 Introduction

The compression capacity of the angle column is strongly affected by its geometry. The non-coincidence of the shear centre with the section's centroid and its location at the intersection of angle legs imply a low torsional stiffness and, therefore, a high susceptibility to instability phenomena involving torsion and flexural buckling about major principal axis, namely flexural-torsional buckling (FTB). Since the FTB deformations exhibited by equal-leg angle columns in the intermediate slenderness domain are very similar to local deformations, these members have been also said to fail in "local-global interactive modes". Besides, the short equal-leg angle columns could be susceptible to the torsional buckling (TB) mode whose failure shape corresponds to the cross-section local buckling (LB). However, the slender equal-leg angle columns will fail due to flexural buckling (FB) mode about minor principal axis of the cross-section.

The difficulty in assessing stability of equal-leg angle columns is especially noticeable in the case of slender, thin-walled sections. The deformation and stress redistribution upon the elastic LB of angle legs reduce effective section properties and cause the effective centroid to shift along the axis of symmetry towards the corner, which, in turn, results in an interaction between the axial load and additional bending. Furthermore, the inevitable presence of initial imperfections and end eccentricity of loading acting in combination with the effective centroid shift additionally affects the occurrence of buckling and subsequent failure. As the cross-section is asymmetric, distribution of axial stresses in the cross-section strongly depends on the direction of total eccentricity along the axis of symmetry—towards the tips of

the legs or to the corner (one causing compressive yielding of the leg tips, the other causing compressive yielding of the section corner). Besides, an increase of the leg width-to-thickness ratio increases the tendency of the angle to rotate and increase possibility for FTB failure in the entire global column slenderness range [1], [2].

This paper briefly present key results of a scientific research addressing cold-formed stainless steel equal-leg angle columns with pin-ended boundary conditions, conducted at the University of Belgrade, Faculty of Civil Engineering, aiming to propose procedures for their design taking into account the cross-section slenderness, material non-linearity and initial structural imperfections caused by particular production process. The analytical background, state of art, experimental procedures, numerical studies and used methodologies are described in detail in recently published papers [1], [2].

2 Experimental programme

The experimental programme was performed on press-braked stainless steel equal-leg angle sections with nominal dimensions of $80 \times 80 \times 4$ mm and nominal internal corner radius of 12 mm, and involved material testing, initial imperfection measurements and stub column tests and global buckling tests. The basic material of all tested angle columns was lean-duplex stainless steel grade EN 1.4162 (UNS S32101) with the steel name X2CrMnNiN21-5-1. The lengths of specimens were selected to cover a wide-ranging set of global column slenderness: elastic LB of short specimens, coupled FTB-LB and FB-LB failure modes for

* Awarded as best young researcher's paper, presented at ASES 2020 Symposium, Arandjelovac, Serbia, May 2021.

* Corresponding author:

E-mail address: jelena@imk.grf.bg.ac.rs

the intermediate and long length specimens, respectively. In order to capture material nonlinearity, the tensile tests were performed on coupons extracted from the final press-braked angle sections under strain-control according to the requirements of EN ISO 6892-1 [3]. Two coupons were longitudinally cut from the middle of a leg, and two from the corner regions, to account for the strength enhancement caused by cold-working. Table 1 lists the average values of key mechanical properties, in which f_y is yield strength taken as the 0.2% proof stress, f_u is the ultimate tensile strength, ϵ_u is the strain corresponding to the ultimate tensile strength, ϵ_f is the total strain at fracture, E is the modulus of elasticity, and n and m are the strain hardening parameters utilised in the Ramberg–Osgood material model for nonlinear metallic materials [4]. It was found that press-braking method significantly improves material strength in the corner regions — the yield strength is about 38% greater than the yield strength of the flat angle section legs.



Figure 1. Typical stub column failure mode [1]

Table 1. Average measured key material properties obtained from tensile coupon tests [1]

Coupon	f_y (N/mm ²)	f_u (N/mm ²)	E (N/mm ²)	ϵ_u (%)	ϵ_f (%)	Strain hardening parameters	
						n	m
Flat leg coupons	517	768	197445	31	45	7.9	3.0
Corner coupons	703	823	199905	17	33	11.0	13.1

The cross-section ultimate resistance and deformation capacity were quantified by stub column tests. A total of three repeated stub column tests were performed under pure axial compression. The nominal length of specimens of 240 mm meets requirements in Clause A.3.2.1 of EN 1993-1-3 [5]. The ends of each specimen were machined flat by a water jet cutter, perpendicular to their longitudinal axes to ensure a uniform distribution of loading during testing. The parallel end plates of the testing machine were fixed against rotations and twist about any axis to achieve fixed boundary conditions. The failure of specimens was governed by local buckling, localised in the middle part of the specimen's height, and characterised by torsional deformations of both angle legs (see Figure 1).

The key experimental results are summarised in Table 2, in which $P_{c,u}$ is the ultimate buckling load, δ_u is the end shortening at ultimate load, σ_{lb} is the LB stress obtained as the ultimate load-to-measured cross-section area ratio of each specimen and f_{ya} is an enhanced average yield strength which accounts for cold working in press-braked sections.

Having established the basic material and cross-sectional response, global buckling tests were carried out on pin-ended angle columns to obtain their compressive resistances and identify key predictors for critical failure modes. The specimens were divided into two test series with nominal lengths of 1000 and 2000 mm and four repeated tests in each of these series. Measurements of specimen geometry and initial global imperfections were performed before tests. A hydraulic testing machine was employed to

apply monotonic compression loading to each column specimens. The load was applied through end plates attached to hardened steel knife-edge devices designed to replicate pinned end conditions, allowing rotations about the minor-axis, while restraining major-axis rotations as well as twist rotations and warping. A data acquisition system was used to record the applied load, lateral displacements (measured by linear variable displacement transducers) and axial strains (measured by strain gauges) during the tests. Table 3 provides relevant data obtained for all tested specimen; $P_{b,u,exp}$ is the maximum axial load capacity of the specimens (compressive column's resistance), $d_{u,v}$ and $d_{u,u}$ are respectively the mid-height lateral deflections about minor and major principal axes, and ϕ_u is the mid-height torsional rotation, all corresponding to the maximum load.

Based on experimental data obtained for global buckling tests, it was conclude following:

- In the intermediate slenderness domain, three repeated specimens failed in an almost identical mode, exhibiting dominant major-axis flexural-torsional deformations, coupled with minor-axis FB and LB, as displayed in Figure 2a. However, the failure of specimen ACF 80 × 80 × 4 – 1000 – 2 was governed by interaction of minor-axis flexural instability FB and local cross-section buckling mode accompanied by significant lateral minor-axis displacements and negligible torsional rotations and major-axis bending (see Table 3).

Table 2. Stub column test results [1]

Specimen	$P_{c,u}$ (kN)	δ_u (mm)	σ_{lb} (N/mm ²)	f_{ya} (N/mm ²)	σ_{lb} / f_{ya}
ACF 80 × 80 × 4 – 240 – 1	199.0	1.21	327.7	544.1	0.60
ACF 80 × 80 × 4 – 240 – 2	198.2	1.17	320.2	544.2	0.59
ACF 80 × 80 × 4 – 240 – 3	203.7	0.83	328.7	544.2	0.60

Table 3. Global buckling test results [1]

Specimen	$P_{b,u,exp}$ (kN)	$d_{u,u}$ (mm)	$d_{u,v}$ (mm)	ϕ_u (deg)
ACF 80 × 80 × 4 – 1000 – 1	132.5	+0.335	+0.339	-8.013
ACF 80 × 80 × 4 – 1000 – 2	139.5	-0.156	+8.149	-0.613
ACF 80 × 80 × 4 – 1000 – 3	136.6	-0.468	+1.471	-6.234
ACF 80 × 80 × 4 – 1000 – 4	135.5	-0.288	+0.846	-8.060
ACF 80 × 80 × 4 – 2000 – 1	44.3	-0.053	+31.487	-0.103
ACF 80 × 80 × 4 – 2000 – 2	45.8	+0.229	+23.948	-0.274
ACF 80 × 80 × 4 – 2000 – 3	46.8	-1.132	+29.094	+0.987
ACF 80 × 80 × 4 – 2000 – 4	45.5	-0.023	+21.972	-0.204

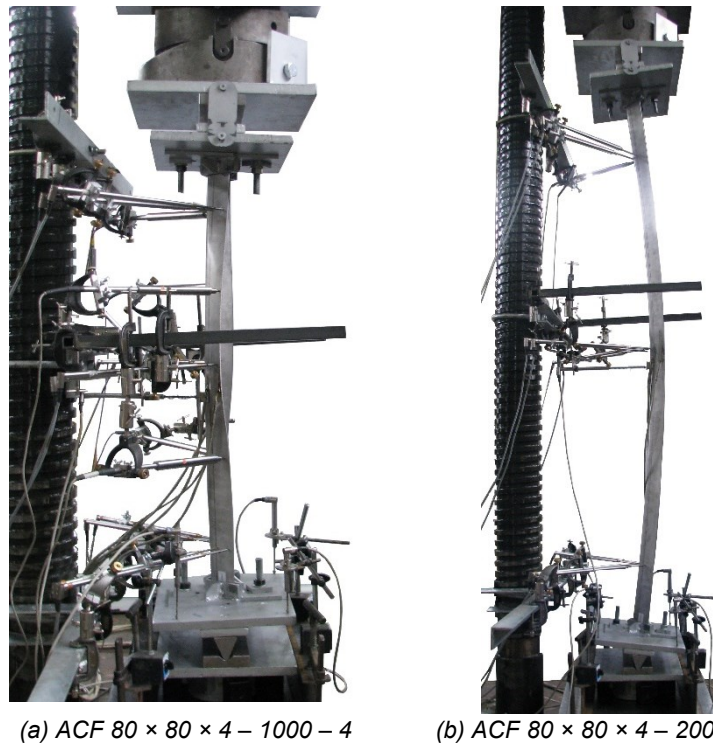


Figure 2. Typical failure modes of intermediate and long length specimens [1]

– As shown in Figure 2b, a dominant failure mode of the long length specimens was global minor-axis FB. The failure pattern involves notable lateral deflections in plane perpendicular to the minor principal axis and negligible twisting in combination with major-axis bending (see Table 3), indicating that the high slenderness specimens are less prone to cross-section LB.

3 Finite element modelling and parametric study

The advanced and realistic numerical simulations of the experiments involved cold-formed equal-leg angle columns were performed using the ABAQUS FE software package [7]. The geometrically and materially non-linear analysis (GMNIA) was developed as quasi-static with the dynamic explicit solver and the variable non-uniform mass scaling technique. The S4R shell elements were used to model the measured geometry of tested columns, as is customary for modelling thin-walled structures. To replicate the realistic pin-ended supporting conditions in global buckling tests, the

measured geometry of hardened steel knife-edge devices attached to steel loading plates, together with top and bottom adjustable clamps were additionally modelled using four hexahedral solid elements C3D8R. A linear elastic-perfectly plastic material model with a nominal plateau slope was used to model material properties of steel end adjustable clamps (S275JR) and the hardened steel knife-edges (S355N). The measured stress-strain curves obtained via flat and corner tensile coupon tests on the lean duplex stainless steel grade EN 1.4162 were used to develop the material models of section' flat legs and corner, respectively. The initial geometric imperfections were explicitly modelled by using lowest local (twist imperfection – local/torsional mode) and global (bow imperfection about the minor-principal axis) buckling modes obtained via Linear Buckling Analysis (LBA) performed on equivalent FE models with the same mesh. The imperfection amplitudes matched the measured ones.

The qualitative comparisons of the failure modes of the intermediate length specimens occurred in the and the FE modelling are presented in Figure 3.

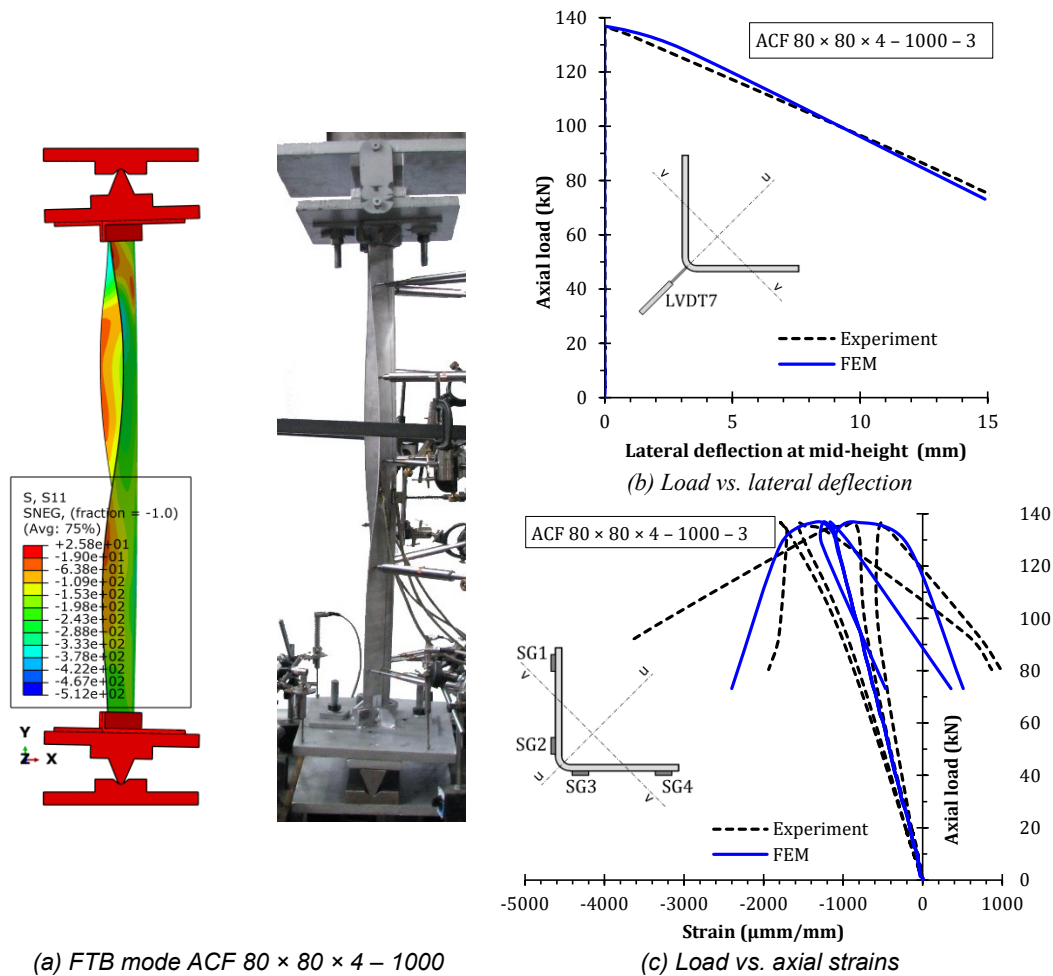


Figure 3. FE model and experimental buckling mode of intermediate length specimens [2]

Experimentally verified nonlinear FE modelling was used to perform an extensive FE parametric study aiming to thoroughly examine the structural responses of cold-formed equal-leg angle columns and develop a database for their reliability-based design. The wide range of columns' global slenderness was considered in the study to investigate LB, major-axis FTB and minor-axis FB resistances. Furthermore, 27 different equal-leg angle sections were selected providing both slender and non-slender cross-sectional behaviour. The influence of material nonlinearity on column ultimate strength was thoroughly analysed for three primary alloys — austenitic, ferritic and duplex stainless steel using collected data from literature [1], [8], [9], [10].

4 Buckling curve proposal and reliability assesment

This section addresses the comparison of the generated experimental [1] and FE data [2] with the design buckling predictions determined in accordance with the procedures described in SRPS EN 1993-1-4 [6] and SRPS EN 1993-1-1 [11]. Figures 4 shows the graphical comparisons of the different European buckling with the FE and test ultimate

loads normalised by the cross-section yield loads for dominant minor-axis FB. The new buckling curve with the imperfection factor $\alpha = 0.92$ and non-dimensional limiting slenderness $\bar{\lambda}_0 = 0.15$ for austenitic data set is also depicted in Figure 4.

Table 4 provides a statistical appraisal of the accuracy of the mentioned procedures considering the mean values of FE & test-to-predicted ratios $N_{b,u}/N_{b,u,pred}$ and the corresponded coefficient of variations (CoVs) per stainless steel grade and per cross-section class. The design predictions of columns with slender angle sections (Class 4) were obtained using interaction equation 5.15 of SRPS EN 1993-1-4 [6], to evaluate the influence of the neutral axis shifting along the major principal axis toward the section corner.

The procedure outlined in Annex D of EN 1990 [12] and the methodology described by Afshan et al. [13] were subsequently performed to assess the reliability of the proposed buckling curves for the cold-formed equal-leg angle columns and calculate the values of the partial factors for member resistance γ_{M1} [6]. The key results of the reliability analysis are also shown in Table 4.

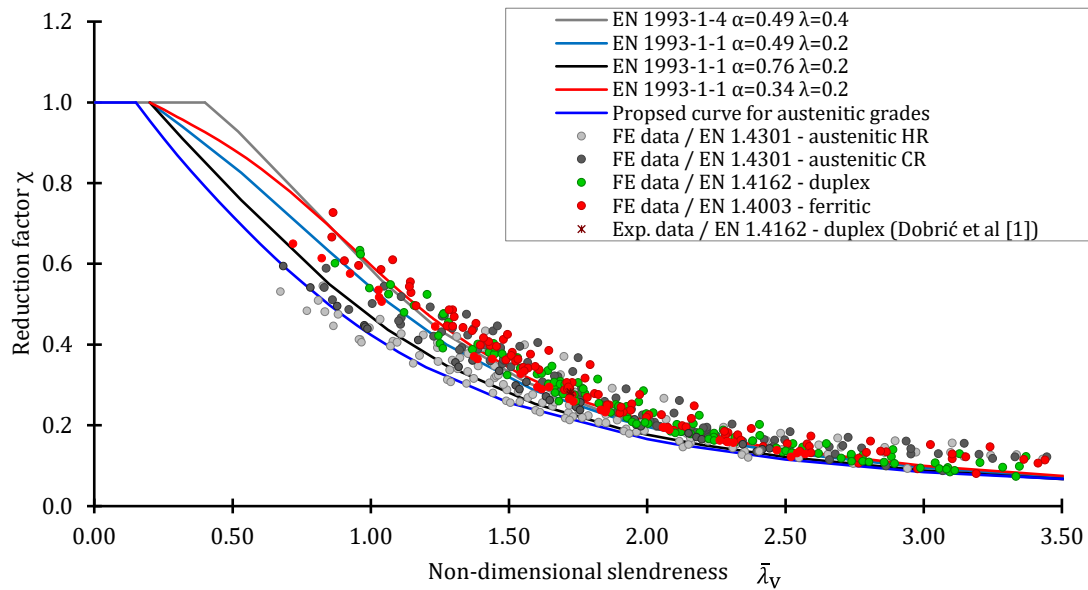


Figure 4. Comparison between normalised FE & test results and European buckling curves for minor-axis FB [2]

Table 4. Comparison between FE & test data and design data and the partial factors for member resistance γ_{M1} obtained in reliability analysis [2]

Grade	Cross-section slenderness	Code	Data no. $\bar{\lambda}_0 > 0.2$	$N_{b,u}/N_{b,u,pred}$		
				Mean	CoV (%)	γ_{M1}
EN 1993-1-4 / minor-axis FB (& minor-axis bending)						
Austenitic	Class 3	$\alpha = 0.76 \quad \bar{\lambda}_0 = 0.2$	98	1.181	27.1	1.21
	Class 4	$\alpha = 0.76 \quad \bar{\lambda}_0 = 0.2 \text{ \& Eq. 5.15}$	193	1.910	40.6	1.21
	Class 3	$\alpha = 0.92 \quad \bar{\lambda}_0 = 0.15$	98	1.198	19.4	1.10
	Class 4	$\alpha = 0.92 \quad \bar{\lambda}_0 = 0.15 \text{ \& Eq. 5.15}$	193	2.001	39.8	1.08
Duplex	Class 3	$\alpha = 0.49 \quad \bar{\lambda}_0 = 0.2$	21	1.007	2.6	1.09
	Class 4	$\alpha = 0.49 \quad \bar{\lambda}_0 = 0.2 \text{ \& Eq. 5.15}$	119	2.054	39.2	1.03
Ferritic	Class 3	$\alpha = 0.49 \quad \bar{\lambda}_0 = 0.2$	49	1.159	21.1	1.09
	Class 4	$\alpha = 0.49 \quad \bar{\lambda}_0 = 0.2 \text{ \& Eq. 5.15}$	85	1.953	38.4	1.09
EN 1993-1-4 / FTB & minor-axis bending						
Austenitic	Class 4	$\alpha = 0.34 \quad \bar{\lambda}_0 = 0.2 \text{ \& Eq. 5.15}$	212	2.892	32.7	1.09
Duplex	Class 4	$\alpha = 0.34 \quad \bar{\lambda}_0 = 0.2 \text{ \& Eq. 5.15}$	104	3.779	28.2	0.67
Ferritic	Class 4	$\alpha = 0.34 \quad \bar{\lambda}_0 = 0.2 \text{ \& Eq. 5.15}$	104	3.373	29.7	0.83

5 Conclusions

A comprehensive investigation of the structural behaviour of cold-formed equal-leg angle columns members under pure compression, including experiments [1] and qualitative and quantitative numerical studies [2], was carried out with the aim of acquiring a valuable database that enabled the development of an accurate and reliable design method. The following conclusions are drawn from this investigation:

- The failure mode of the short equal-leg angle specimens was governed by elastic local buckling akin to TB, occurring at a stress value that is 40% lower than the measured average yield strength. Elastic FTB coupled with LB and minor-axis FB was the dominant failure mode for

specimens in the intermediate slenderness domain. In the high slenderness domain, the failure mode of all specimens was minor-axis FB. The test results also indicate that the long length specimens were not prone to LB.

- Considering the austenitic dataset, comparisons of the test & FE resistances with design predictions obtained for buckling curve d ($\alpha = 0.76 \bar{\lambda}_0 = 0.2$), demonstrate that the European design method may be either conservative for slender sections (Class 4) or even excessively unconservative, particularly for non-slender sections (Class 3). The unsafe predictions are more significant for columns made from austenitic hot-rolled strips which have noticeably lower structural responses in comparison with their counterparts produced from cold-rolled austenitic strips. Thus, the buckling curve d offer unsatisfactory design

predictions with the safety factors γ_{M1} significantly higher than the currently adopted value of 1.10.

- The proposed buckling curve ($\alpha = 0.92$ $\bar{\lambda}_0 = 0.15$) offers improved fit to available data, providing a higher average ratio of the test & FE resistance-to-design resistance and less scatter across the austenitic datasets both for slender and non-slender angle sections, in comparison with the Eurocode buckling curve *d*. The safety factors γ_{M1} are equal to 1.10 and 1.09 for non-slender (Class 3) and slender (Class 4) angle sections, respectively.

- In contrast to austenitic grade, the predictive curve *c* ($\alpha = 0.49$ $\bar{\lambda}_0 = 0.2$) is in good agreement with FE & test data for duplex and ferritic grades. The safety factors γ_{M1} are lower than 1.10 for all cross-section classes.

- The FTB response of cold-formed equal-leg angles is strongly associated with their cross-section dimensions. The increasing of the leg slenderness leads to appearing of elastic local buckling accompanied by the torsional rotations of angle section. The comparative analysis shows that the European design method covering the interaction of FTB and uniaxial minor-axis moment gives safe but significantly conservative predictions and safety factors lower than 1.10 for all three stainless steel grades.

Funding and Acknowledgements

This investigation is supported by the Serbian Ministry of Education, Science and Technological Development through the TR-36048 project.

The authors are grateful to companies Montanstahl ag Switzerland, Vetroelektrane Balkana Belgrade, Armont SP Belgrade, Institute for Testing of Materials Belgrade, Institute for Materials and Structures Faculty of Civil Engineering University of Belgrade, ConPro Novi Sad, Energoprojekt Industrija PLC Belgrade, Vekom Geo Belgrade, CO-Designing, Peri Oplate Belgrade, North Engineering Subotica, Amiga Kraljevo, Mašinoprojekt kopriv PLC Belgrade, Sika Belgrade, DvaD Solutions Belgrade and Soko Inžinjering Belgrade for their support.

References

- [1] Dobrić J, Filipović A, Marković Z, Baddoo N.: Structural response to axial testing of cold-formed stainless steel angle columns, *Thin-Walled Structures*, 156, 2020.
- [2] Dobrić J, Filipović A, Baddoo N, Marković Z, Buđevac D.: Design procedures for cold-formed stainless steel equal-leg angle columns, *Thin-Walled Structures*, 107210, 2020.
- [3] EN ISO 6892-1. Metallic materials – Tensile testing. Part 1: Method of test at room temperature. Brussels, Belgium, CEN 2009.
- [4] Arrayago I, Real E, Gardner L.: Description of stress-strain curves for stainless steel alloys, *Materials and Design*. 2015;87:540-552.
- [5] Eurocode 3: Design of Steel Structures – Part 1-3: General rules - Supplementary rules for cold-formed members and sheeting EN 1993-1-3, Brussels, Belgium, CEN 2006.
- [6] Eurocode 3: Design of steel structures – part 1-4: General rules – supplementary rules for stainless steels, including amendment A1 (2015), EN 1993-1-4:2006+A1:2015, Brussels, Belgium, CEN 2015.
- [7] ABAQUS User Manual. Version 6.12. Providence, RI, USA: DS SIMULIA Corp; 2012.
- [8] Dobrić J, Buđevac D, Marković Z, Gluhović N.: Behaviour of stainless steel press-braked channel sections under compression, *J. Construct. Steel Res.* 139 (2017) 236–253.
- [9] Lecce M, Rasmussen K.J.: Distortional Buckling of Cold-Formed Stainless Steel Sections: Experimental Investigation, *J Struct Eng., ASCE* 132 (4) (2006) 497–504.
- [10] Rossi B, Jaspart J.P, Rasmussen K.J.: Combined distortional and overall flexural-torsional buckling of cold-formed stainless steel sections: Experimental investigations, *Journal of Structural Engineering*. 136 (4) (2010) 354–360.
- [11] Eurocode 3: Design of steel structures – Part 1-1: General rules and rules for buildings EN 1993-1-1, Brussels, Belgium, CEN 2005
- [12] Eurocode: Basis of structural design EN 1990, Brussels, Belgium, European Committee for Standardization (CEN); 2002.
- [13] Afshan S, Francis P, Baddoo N.R, Gardner L.: Reliability analysis of structural stainless steel design provisions, *J. Construct. Steel Res.*, 114 (2015) 293–304.